Vibration isolation for gravitational wave detection

Class. Quantum Grav. 10 (1993) 2407–2418. Printed in the UK

Vibration isolation for gravitational wave detection

D G Blair, L Ju and H Peng

Department of Physics, University of Western Australia, Nedlands, Western Australia 6009, Australia

Received 2 November 1992, in final form 20 May 1993

Abstract. Through a combination of experiment and numerical modelling, we show that vibration isolators using cantilever springs can be used to achieve vibration levels below 10^{-20} m/$\sqrt{}$Hz for frequencies above 100 Hz, and that this performance can probably be achieved for frequencies as low as 25 Hz. Damping of high Q normal modes in all metal isolator structures can be relatively easily achieved by a combination of active and narrow band eddy current damping while the use of a single-stage ultra-low-frequency pre-isolator can eliminate the need for such damping. Utilizing an improved sapphire transducer, new measurements of the isolator's performance are presented. The measurement noise floor reaches 10^{-15} m/$\sqrt{}$Hz for vertical displacements and 10^{-14} m/$\sqrt{}$Hz for horizontal displacements.

PACS number: 0480

1. Introduction

Predicted sources of gravitational waves in the 10 Hz to 10 kHz range have strain amplitude $h \sim 10^{-20}$. Rare signals could be as strong as 10^{-18}, while frequent events can be expected at the sensitivity goal $h \sim 10^{-23}$ of large scale laser interferometer detectors (LIDs). In practice both metre-scale detectors (resonant bars) and kilometre-scale detectors must be able to register displacement amplitudes $\sim 10^{-20}$ m to achieve their sensitivity goals ($h \sim 10^{-20}$ and 10^{-23} respectively).

In the frequency range 1 Hz to 10^3 Hz ground vibration amplitudes are typically given by $x = kf^{-2}$ m Hz$^{-1/2}$, where k varies from $\sim 10^{-6}$ at a bad urban site to $\sim 10^{-8}$ in underground sites. It is therefore necessary to attenuate ground vibrations by 8–10 orders of magnitude of 100 Hz.

A simple vibration isolator is a mechanical low-pass filter. While attenuating high-frequency vibration, without care it can resonantly amplify low-frequency vibration. Traditional isolators consist of a stack of alternating masses and damped springs, usually made of rubber. However, damping introduces thermal noise and rubber has poor vacuum performance and poor dimensional stability.

The N normal modes of an N-stage isolator are distributed below the cut-off frequency, depending on the individual masses and spring constants chosen, as shown in the figures below. The low-pass cut-off frequency is usually about twice the single mass–spring frequency of the isolator elements. To operate in the high vacuum of an LID, it is convenient if the isolator is made of all metal components. This means that the normal modes may have relatively high Q factors ($\sim 10^2$–10^3). The isolator is a complex system of coupled resonators, so the Q-value of each normal mode depends

on the losses of all of the elements. Some normal mode amplitudes may be many orders of magnitude higher than the background seismic noise. This can lead to many practical difficulties.

In a laser interferometer detector the optical cavities or delay lines must be accurately locked to the laser light. Servo control is greatly simplified if the mirror velocities are low. Long term drifts due to temperature variation or creep will also be a problem for long term operation. Thus rubber is best avoided. All metal isolator structures should be superior except for the problem of resonant enhancement of the normal modes.

An additional problem affecting coastal sites above ground is the existence of a micro seismic noise peak at about 0.2 Hz, caused by ocean waves. The peak can reach about 30 μm amplitude, and since the seismic wave velocity is low ($\sim 300\ \mathrm{m\ s^{-1}}$) the signal can be uncorrelated between the arms of a 3 km interferometer. The velocity amplitude may be as great as $30\ \mu\mathrm{m\ s^{-1}}$ [1]. To overcome this problem some vibration isolation at about 0.1 Hz is advantageous.

With these constraints in mind, we show in this paper that isolators can be optimized using a variety of techniques. Resonant enhancement of the normal modes can be minimized by use of active reaction force damping and magnetic resonant absorbers. Alternatively, ultra-low-frequency pre-isolation can minimize seismic excitation of these modes. We show that a judicious mix of these methods can be used to create isolation systems which are suitable for use in high vacuum environments, and which can give isolation performance superior to that originally anticipated for LIDs. We show that noise levels below $10^{-20}\ \mathrm{m\ Hz^{-1/2}}$ can be expected for frequencies above 100 Hz, and demonstrate performance to $10^{-15}\ \mathrm{m\ Hz^{-1/2}}$. (The level is set by the noise floor of the sapphire transducer used in the tests.) Model results demonstrate the advantage of using ultra-low-frequency pre-isolators, and we propose a configuration utilizing negative springs which would be suitable.

2. Damping methods for multistage isolators

We have studied damping techniques on an all-metal multistage isolator with cut-off frequency ~ 40 Hz vertically and ~ 20 Hz horizontally. These use steel masses and cantilever springs, and are described in [2]. Each stage uses a 40 kg disc and a star shaped spring structure with a 22 Hz natural frequency. Figure 1 shows typical normal mode response curves. There is good agreement between theoretical and experimental performance. It is also evident that there is cross-coupling between the vertical and horizontal responses. This creates a shoulder in the horizontal response data about two orders of magnitude below the horizontal normal modes.

It is useful to consider the possible damping techniques available to reduce normal mode amplitudes. First we considered the use of *lossy metals*. The well known low-Q metals such as lead could be utilized to reduce the Q-factor of springs. The low Q of lead arises from an acoustic loss peak near room temperature. This is strongly temperature-dependent, and reduces the Q factor to about 30. We have investigated the use of cantilever springs coated with a thick layer of lead [3]. Unfortunately, because a large mass of low loss material is required to maintain the strength of the spring, we find this technique to be unsatisfactory. It is very difficult to achieve Q-factors below 100.

A more elegant approach is to use *magnetic eddy current damping*. In an LID, the uncertainty principle requires the test masses to be ~ 1 t. Thus isolators must be designed

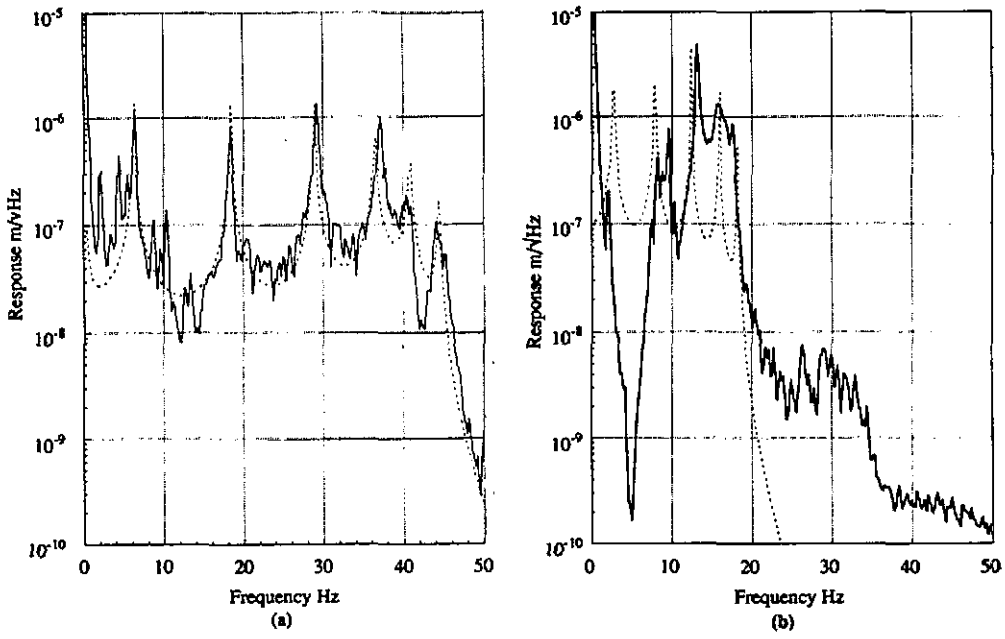

Figure 1. Comparison of theoretical and experimental response curves of five-stage isolator driven with white noise. (*a*) Vertical response and (*b*) Horizontal response. The solid lines are experimental results and the dotted lines are the theoretical ones. Note that the horizontal experimental response has a shoulder between 20 Hz and 35 Hz due to a cross-coupling of the vertical normal modes at about 10^{-2} of their amplitude.

to support such loads. We have found that magnetic eddy current damping using high field NdFeB magnets moving near copper conductors can exceed critical damping when the conductor mass is less than about 10 times the magnet mass. For 1 t test masses and comparably massive isolator elements, the cost and complexity of direct magnetic damping make this an impractical approach. An alternative method of magnetic damping utilizes the *narrow band resonant absorber* [4]. In this case individual modes of an isolator can be damped using a magnetically damped tuned resonator of reduced mass. A low-mass resonator is attached to the isolator in a position where it couples well to the mode of interest. We have used a cantilever spring resonator with copper masses. NdFeB magnets are mounted near to the copper mass. The resonator exchanges energy with the relevant isolator mode, while its mass is low enough that it does not significantly alter the isolator dynamics. The Q-factor of the chosen mode can be tuned by adjustment of the magnet–copper spacing. Such an absorber is able to lower the Q-factor of a normal mode to a value given by

$$Q = \sqrt{\frac{2}{3}\left(\frac{1+\mu}{\mu}\right)^3} \tag{1}$$

where $\mu = m/M$ is the mass ratio of the absorber and vibrating element.

Figure 2 shows the arrangement of the narrow band vibration absorber and figure 3 shows the effect of one damped absorber tuned to the lowest vertical resonant peak.

In this way we have been able to reduce the resonant excitation of the lower normal

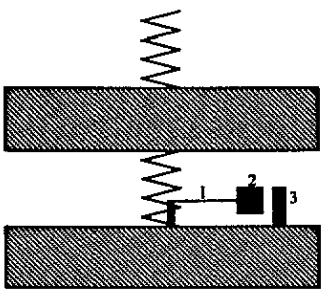

Figure 2. Narrow band damped absorber arrangement, showing the cantilever spring (1), the copper mass (2), and an NdFeB magnet for damping (3).

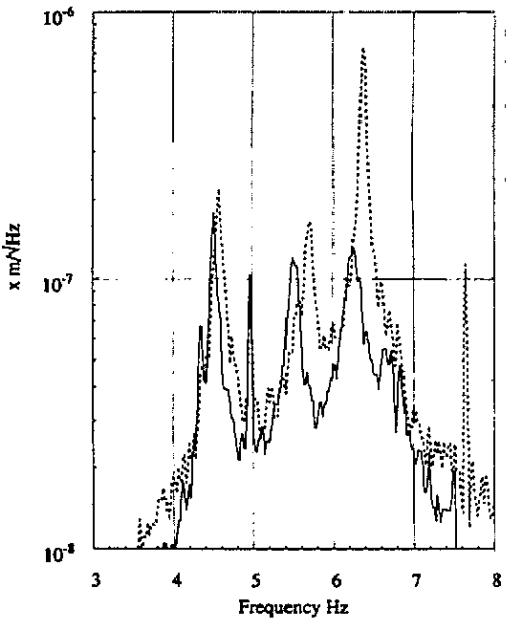

Figure 3. Spectral response of a narrow band magnetically damped vibration absorber tuned to the 6.4 Hz normal mode of a five-stage 22 Hz isolator. The absorber is mounted on the fourth mass where the amplitude of the first mode is largest. The dotted curve shows the original amplitude, without absorber. The solid curve shows that the 6.4 Hz mode amplitude is reduced from $\sim 10^{-6}$ m Hz$^{-1/2}$ to about 10^{-7} m Hz$^{-1/2}$. The scatter in the data is due to time variations in seismic noise.

modes of an isolator (at 6.4 Hz and 18.2 Hz) to within an order of magnitude of the seismic noise background.

An alternative approach is to use *active damping*. The motion is sensed with an accelerometer, and a force is fed back to the isolator with a phase appropriate for damping the motion. For conventional engineering applications, the force transducer is mechanically referenced to the ground. This is undesirable in our case, as this would introduce seismic noise which would effectively short circuit the isolator. For this reason a reaction force method is preferable, and the forces are applied relative to an inertial mass. The device is effectively an inverse accelerometer. We use a loudspeaker with the reaction mass of the cone increased to about ~ 0.1 kg. The arrangement of active damping was described in [2]. In practice, reaction force damping works better at higher frequencies because the finite mechanical range of the driver (about 10 mm) causes the maximum applied force to reduce quadratically as the frequency falls to zero.

Using a combination of resonant absorption for the lower modes and active reaction-force damping for the higher modes we are able to reduce the amplitude of the normal modes in a five-stage isolation stack to less than $\sim 10^{-7}$ m (figure 4). The peak velocity (which occurs for the first and third modes) is reduced to $< 2\ \mu$m s^{-1}.

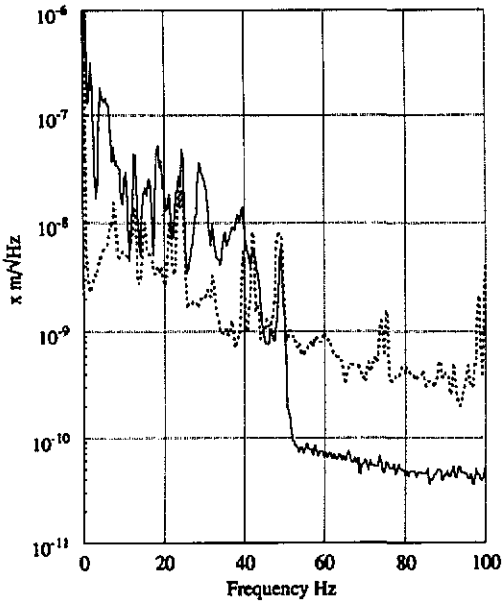

Figure 4. Comparison of seismic noise measured on the laboratory floor (dotted curve) and the normal mode response of a five-stage isolator (solid curve) when active and passive damping are applied. Above 50 Hz the measurement on the isolator is limited by the noise floor of the geophone used for the measurements.

This isolator, when combined with a single pendulum to suspend the test-mass mirrors in an LID, would achieve reasonable performance above 100 Hz. This is discussed in section 3.

While these results are satisfactory, we now show that an alternative approach—the use of a single *ultra-low-frequency* (ULF) *pre-isolation stage*, if it could be realized, would be preferable. In the ideal case one such stage would replace all multistage isolators. Realistically, the ULF stage (incorporating either active or passive damping of its single low-frequency normal mode) would eliminate the normal mode problems in a conventional isolation stack, and also provide isolation against the microseismic noise peak. In section 4 a practical design for such an isolator is discussed.

3. Comparison of isolation configurations

To explore new isolator configurations, we use computer modelling methods to compare various isolator configurations. In particular, we consider the advantages of low-frequency (LF) stages (e.g. a pendulum with frequency ~ 1 Hz) and ULF stages in various combinations with or without the mid-frequency (MF) isolation stacks discussed above. In this analysis it is critical to include both the thermal noise and the seismic noise contribution to the isolator response. Finally, we include a non-ideal but more realistic response for the ULF stage.

Figure 5 shows the response of several hypothetical isolators. In all cases we assume that the isolator is driven by $10^{-6} f^{-2}$ m $\mathrm{Hz}^{-1/2}$ seismic noise (a conservative estimate) above 1 Hz, white seismic noise of amplitude 10^{-6} m $\mathrm{Hz}^{-1/2}$ below 1 Hz and thermal

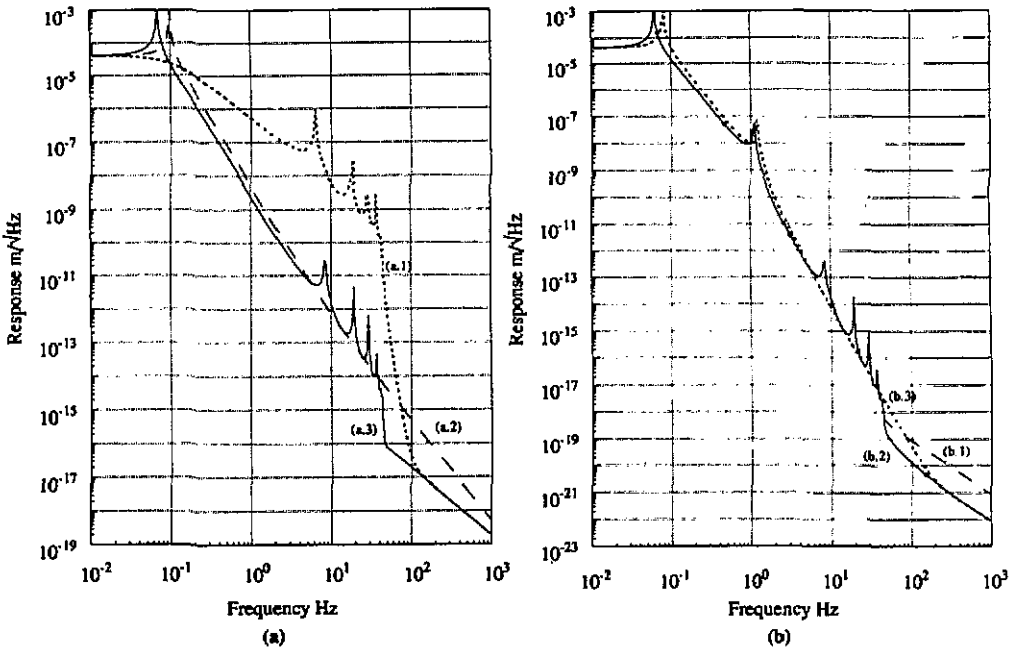

Figure 5. Comparison of the responses of different isolator configurations. (*a*) Comparison of the responses of a five-stage MF isolator with and without a ULF stage. (a.1)—five MF stages ($f_0 = 22$ Hz, $Q_{all} = 10^3$); (a.2)—a single ULF stage ($f_0 = 0.1$ Hz, $Q = 10^2$); (a.3)—a ULF stage followed by five MF stages. (*b*) Isolation responses with a 1 Hz pendulum for the final stage. (b.1)—a ULF stage ($f_0 = 0.1$ Hz, $Q = 10^2$) followed by five MF stages ($Q_{all} = 10^3$) plus a 1 Hz pendulum ($Q = 10^6$); (b.2)—the pendulum Q-factor is increased to 10^8; (b.3)—a ULF stage ($f_0 = 0.1$ Hz, $Q = 10^2$) directly followed by a 1 Hz pendulum ($Q = 10^6$).

noise at room temperature. Curve (a.1) shows the response of a five-stage MF isolator of the type discussed in section 2 ($f_0 = 22$ Hz, $Q_{all} = 10^3$). Curve (a.2) gives the response of a single-stage 10^{-1} Hz isolator with a Q-factor of 10^2, curve (a.3) a single-stage 10^{-1} Hz isolator with a $Q = 10^2$ followed by a percentage stage MF isolation stack the same as in curve (a.1). The ULF isolator clearly gives an enormous advantage in that both thermal noise and isolation are extremely good above several tens of Hz. Somewhat better performance can be regained if the isolator of curve (a.3) has added to it a pendulum with $Q \sim 10^6$, as shown in curve (b.1), and this can be further improved if the pendulum Q is increased to 10^8 (curve (b.2)). However, a ULF stage followed by a 1 Hz pendulum with $Q = 10^6$ (curve (b.3)) is superior to the ideal ULF stage alone.

Comparing curves (b.1) and (b.3), there is little advantage in adding an MF stack to an ideal ULF stage. The above results would imply a very simple solution to the vibration isolation problem if a high-Q ULF stage could be realized and used in conjunction with a high-Q 1 Hz pendulum. Unfortunately it is probably impossible to achieve such ideal performance because of the presence of internal modes and acoustic transmission paths in any large structure which could have the desired ULF resonance. This is an example of a rather general rule that low-pass filters, whether mechanical or electrical, cease to maintain their performance as they cross the transition region from low frequencies where they can be modelled and constructed in terms of lumped circuit parameters to frequencies where their distributed nature dominates. The breakdown occurs first at the

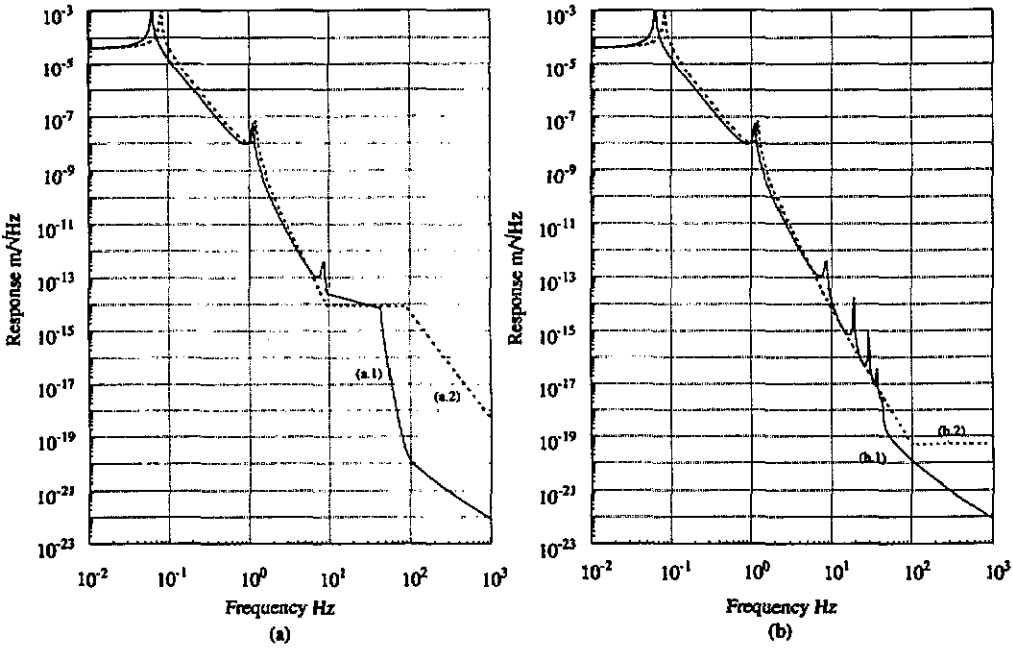

Figure 6. Isolator responses for configurations in which the ULF stage is short-circuited above some cut-off frequency. The parameters of the system are as follows: ULF stage; $f = 0.1$ Hz, $Q = 10^2$, *five-stage* MF *stack*; $f_0 = 22$ Hz, $Q_{(\text{allstages})} = 10^3$, *high-Q pendulum*; $f = 1$ Hz, $Q = 10^8$. (*a*) The ULF stage is short-circuited at 10 Hz. (*b*) The ULF stage is short-circuited at 100 Hz. Note that if the first internal resonance occurs at 100 Hz, there is practically no degradation of performance. For comparison, the dotted lines in both diagrams are the response of a ULF stage plus a pendulum only, without the five-stage MF isolator.

frequency of the lowest *internal* mode, and becomes progressively more serious as the mode density increases.

We now discuss the implementation of a ULF isolator. For the models we have considered, the first internal modes will occur between 10–100 Hz. Above this point the internal modes will contribute their own thermal noise, and will strongly transmit seismic noise. We model this by assuming a high-pass cut-off, between 10 Hz and 100 Hz. Figure 6 shows the isolator response in this case. It is now apparent that best performance will be achieved if an MF stack and pendulum stage are included. The MF stack provides isolation against the non-ideal feedthrough of the ULF stage, and the 1 Hz stage provides the final high-Q suspension. The final response achieved depends on the cut-off frequency of the ULF stage, and the Q of the final pendulum stage.

Figure 7 shows the final achievable response of the isolation configuration as described above shown in the region of greatest interest, along with the photon shot noise limit estimated previously in [5]. The dotted curve shows the degraded performance if the ULF stage is short-circuited after 10 Hz by internal resonances. The configuration proposed here gives a significant additional margin in low-frequency response, compared with isolation configurations proposed for the LIGO and GEO projects [6, 7]. This could be very valuable in the identification of binary coalescence events, because it allows observations at frequencies where the rate of change of frequency is much slower.

It is interesting to ask what ultimate low-frequency behaviour could be achieved.

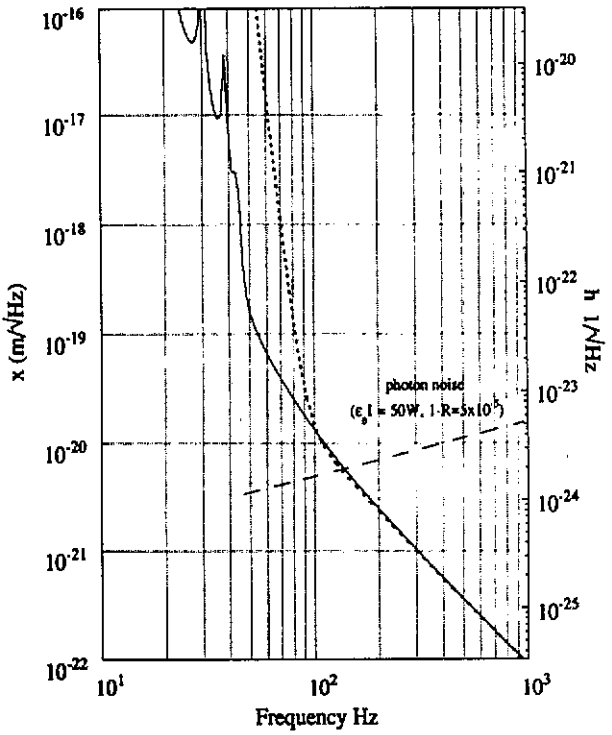

Figure 7. Isolation achievable in a 3 km interferometer using an ultra-low-frequency stage ($Q = 10^2$) along a five-stage 22 Hz stack ($Q = 10^3$), followed by a high-Q ($Q = 10^8$) pendulum isolation along with photon noise. The dotted curve is the case when the first internal resonance of the ULF stage occurs at 10 Hz.

We have tested cantilever stages with resonant frequency ~ 2 Hz [8]. Final stage pendulum suspension could achieve $Q \sim 10^{10}$ [9]. An isolator with five 2 Hz stages, combined with a ULF stage and a pendulum of $Q \sim 10^{10}$ would have the performance shown in figure 8. There is little advantage of having more than five 2 Hz stages. Further details of the design of such an isolator will be published elsewhere.

4. Practical ULF stage

We consider here ways of implementing an ultra-low-frequency stage. Giazotto *et al* [10] have experimented with gas springs, and have achieved very low cut-off frequencies. An alternative method is the use of negative springs. These can be implemented in one or two dimensions using either magnetic repulsion or gravity (the inverse pendulum) to provide a negative spring constant to cancel the internal spring constant of a simple resonator. A similar system has been proposed by Giazotto *et al* [11]. Taking the inverse pendulum as an example, the angular frequency is given by

$$\omega = \sqrt{\frac{k}{m} - \frac{g}{l}} \tag{2}$$

where k is the spring constant of a vertical (inverse pendulum) cantilever spring, m is

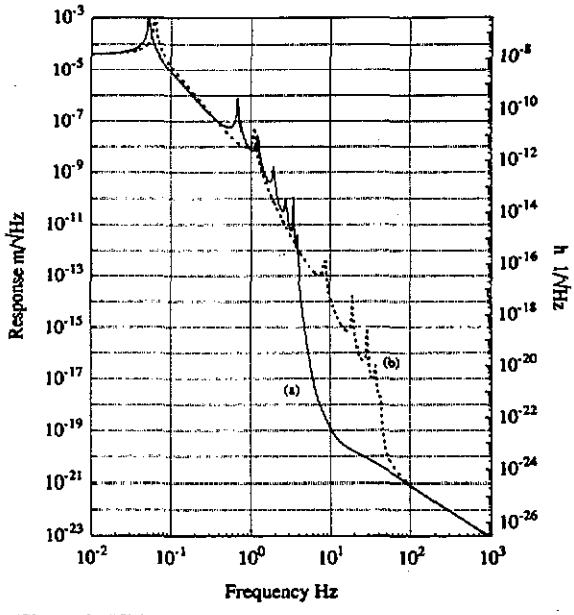

Figure 8. Ultimate isolation performance by using an ultra-low-frequency stage (f = 0.1 Hz, $Q = 10^2$) and a five-stage 2 Hz stack ($Q_{1\sim4} = 10^3$, $Q_5 = 10^6$), followed by an ultra-high-Q pendulum (f = 1 Hz, $Q = 10^{10}$). The dotted curve is that with five 22 Hz mid-frequency stages. The high Q-factor for element 5 of the 2 Hz stack is necessary to prevent thermal noise from this stage from degrading overall performance.

its mass, g is the acceleration due to gravity and l is its length. In this case $\omega \to 0$ as $m \to kl/g$.

Using these principles we have reduced the resonant frequency of a 60 cm high horizontal platform from a few Hz (at zero mass loading) to 0.14 Hz. Using this method we are confident that by adding active control to a larger scale structure, we can reduce the resonant frequency to between 10^{-1} and 10^{-2} Hz, while maintaining reasonable stability. A comparable vertical stage has been designed using torsion bar springs and NdFeB magnets in repulsion to provide a negative spring constant. When combined, these stages can provide three-dimensional isolation from 10^{-1} Hz to 100 Hz. Figure 9 shows a simplified diagram of such an isolator, which could have the isolation characteristic shown in figure 6(*b*), but this could be degraded to figure 6(*a*) if the first internal resonances occur at 10 Hz.

5. Noise floor measurement using a sapphire transducer

The sapphire transducer is an extremely sensititive accelerometer which has been described elsewhere [12]. However, it has a dynamic range of only 10^{-7} m. To prevent the low-frequency normal modes from saturating the transducer, we have used a test mass mechanical resonant frequency of 210 Hz so that it is comparatively insensitive to the (less than 210 Hz) normal modes of the isolator. This greatly increases the noise floor below 200 Hz but allows a wider dynamic range to be achieved. In addition, two additional low-freqency stages were added to the five-stage isolator. The first, acting as

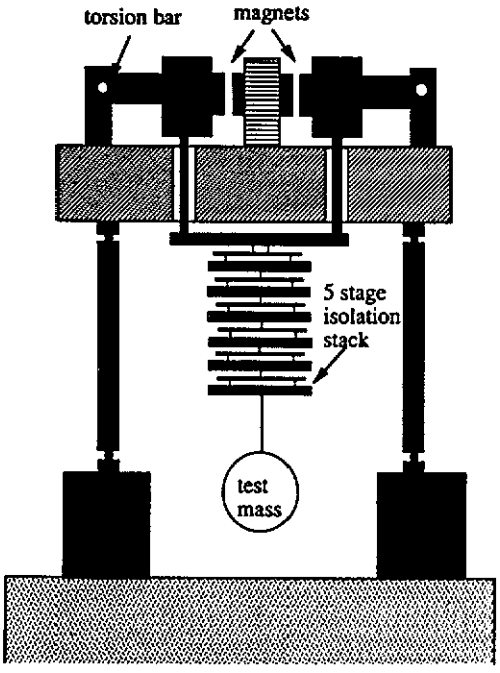

Figure 9. Simplified diagram of a proposed 10^{-1} Hz isolator consisting of a horizontal stage based on an inverse pendulum, and a vertical stage using torsion bars and negative magnetic springs. Four pillars have flexure regions at the top and bottom to create the inverse pendulum. The magnets are set in repulsion to create a magnetic negative spring to balance against the torsion bar.

a pre-isolator, is a 2 Hz vertical spring which suspends the entire experiment (including the vacuum system), while the second, a 1 Hz pendulum, is attached at the bottom of the isolator to provide horizontal attenuation of the normal mode resonant peaks. Data were taken in separate runs with the transducer set up first vertically and then horizontally. In each case the microwave readout system for the transducer was different, and the noise floors achieved were 10^{-15} m $Hz^{-1/2}$ for the vertical system, and 10^{-14} m $Hz^{-1/2}$ when set horizontally as shown in figure 10. The sharp peaks on the noise floor are due to the microwave system which pumps the sapphire transducer. The only real signals visible are below 50 Hz.

Using narrow band excitation at a level of about 40 dB above seismic noise, there is no detectable vertical or horizontal signal from the sapphire transducer above 500 Hz. Between 200 Hz and 500 Hz, a 300 Hz vertical resonance and 490 Hz horizontal resonance were observed under such excitation. However, we believe that these two peaks were due to mechanical vibration of one component of the microwave signal recovery system, and are not due to transmission in the isolator.

To our knowledge the sapphire transducer is the most sensitive non-cryogenic local inertial sensor ever developed. However, these tests only demonstrate that the isolators do not have any serious failings. The 10^{-15} m $Hz^{-1/2}$ noise floor is still well above the expected performance level of the isolator, and only a gravitational wave detector readout system will be able to confirm this performance to full specifications. The narrow band excitation measurements demonstrate that the isolators behave linearly. Non-linear up-conversion is not a problem and the 40 dB excess seismic noise can be used

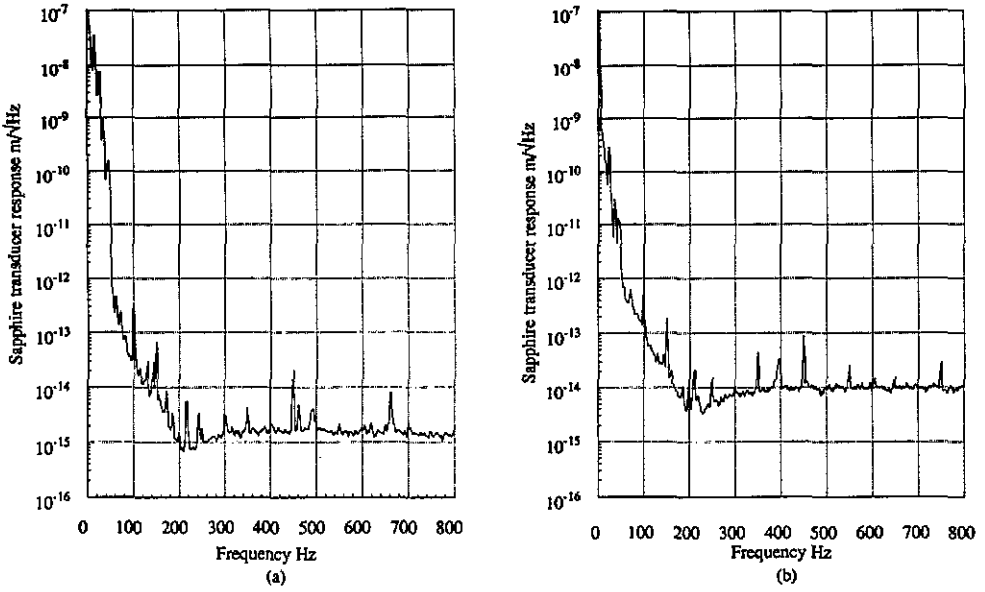

Figure 10. Performance of the isolator. (*a*) Vertical response. (*b*) Horizontal response. The only data which represents real seismic signals and not the transducer noise floor is for frequencies below 50 Hz.

to extrapolate the isolator performance to 10^{-17} m $Hz^{-1/2}$, still three orders of magnitude above the expected design performance.

6. Conclusion

Isolation systems for laser interferometer gravitational wave detectors could be improved by the use of ultra-low-frequency isolation stages using negative springs to achieve corner frequencies of the order of 0.1 Hz. Passive absorption damping or reaction force damping can be harnessed to reduce the effective Q-factors of the normal modes in mid-frequency isolators to about 10. However, a single high-Q pendulum stage is still necessary to reduce the thermal noise in the last stage of the isolator. A proposed isolator configuration allows the strain sensitivity of a 3 km interferometer to reach 10^{-23} $Hz^{-1/2}$ for frequencies above 100 Hz. An isolator consisting of a ULF stage combined with a five-stage 2 Hz cantilever spring mass system and a very high-Q pendulum ($Q = 10^{10}$) could achieve the same sensitivity down to 25 Hz. Local measurements on one isolator using a sapphire transducer show no excess vibration above the 10^{15} m $Hz^{-1/2}$ noise floor of the transducer. Excitation measurements allow this to be extrapolated to 10^{-17} m $Hz^{-1/2}$. Further work will test the operation of the isolator in an 8 m Michlson interferometer, and will use lower normal mode frequencies.

Acknowledgments

We wish to thank Frank van Kann for the computer program used to model the isolators, Mark Pinoli for testing the prototype inverse pendulum isolator, and Peter Turner and Ron Bowers for invaluable assistance.

References

[1] Blair D G, McClelland D E and Bachor H 1992 *Austral. New Zealand Physicist* **29** 64
[2] Ju L, Blair D G, Peng H and van Kann F 1992 *Meas. Sci. Technol.* **3** 463
[3] Blair D G, van Kann F J and Fairhall A L 1991 *Meas. Sci. Technol.* **2** 846
[4] Rao J S and Gupta K 1984 *Introductory Course on Theory and Practice of Mechanical Vibration* (New York: Wiley)
[5] Drever R W P 1991 *The Detection of Gravitational Waves* ed D G Blair (Cambridge: Cambridge University Press)
[6] Abramovici A *et al* 1992 *Science* **256** 325
[7] Hough J 1989 *Prospects for Gravitational Wave Detectors with Laser Interferometer Detectors, Proceedings of the Fifth Marcel Grossmann Meeting* ed D G Blair and M Buckingham (Singapore: World Scientific)
[8] Blair D G and Ju L Low frequency cantilever spring vibration isolators, to be published
[9] Blair D G, Ju L and Notcutt M 1993 *Rev. Sci. Instrum.* **64** 1
[10] Fabbro R D *et al* 1988 *Rev. Sci. Instrum.* **59** 293
[11] Giazotto A private communication
[12] Blair D G, Ivanov E N and Peng H 1992 *J. Phys. D: Appl. Phys.* **25** 1110